Design of Compact Vertically Stacked SIW End-Fire Filtering Antennas with Transmission Zeros

Changzhou Hua*, Xiangyu Jin, and Meng Liu

Abstract—This paper presents a new type of vertically stacked substrate integrated waveguide (SIW) filtering antenna. It is composed of an SIW bandpass filtering circuit and an antipodal linearly tapered slot antenna (ALTSA). The filtering circuit consists of two vertically stacked SIW cavity resonators which are coupled with each other by etching slot on the common metal layer. By introducing electric and magnetic mixed coupling structures, close-to-passband transmission zeros can be realized and flexibly adjustable. Due to the partially vertically stacked structure, the proposed filtering antenna also shows a compact physical size. For validation, two vertically stacked SIW filtering antennas operating at 30 GHz with transmission zero at the upper or lower side of the passband are designed, fabricated, and measured. Good agreement is observed between the measured and simulated results.

1. INTRODUCTION

With the rapid development of wireless technology, high integration and miniaturization of radio frequency (RF) front-ends are becoming more and more noticeable. Filters and antennas are critical components in RF front-ends. Traditionally, the filter and antenna are designed separately, which usually causes large size and impedance mismatch. And the performances of the filter and antenna may also be deteriorated. In recent years, filtering antenna has become an interesting topic [1]. By integrating filtering circuits into conventional antennas, researchers developed the co-designed filtering antennas. Various filtering antennas have been realized by integrating additional or embedded filtering circuits to the antenna feeding networks [2–8]. A second-order filtering microstrip antenna with quasi-elliptic function antenna gain response was presented in [2]. By introducing two radiation nulls, a pair of steep skirt at passband edge was obtained. In [3], a half-mode substrate integrated waveguide (SIW) cavity resonator was used in conjunction with a conventional SIW cavity to obtain a single-layer two-pole filtering antenna design. By using a printed Jerusalem-cross radiator and a ring slot-coupled feed structure, a filtering antenna without extra filtering circuits was presented in [4], provides both good filtering and dual-polarized radiating performances. A reconfigurable circular polarization (CP) filtering antenna was proposed and studied in [5], which was capable of switching its polarization between left-hand CP and right-hand CP by using PIN diodes. In order to further reduce the footprint of the RF front-ends, slot antennas integrated with vertical cavity filters were demonstrated [6, 7]. However, the previously reported filtering antennas were mostly focused on broadside radiations, filtering antenna with end-fire radiations has been rarely reported. In [8], a differential end-fire filtering quasi-Yagi antenna was exhibited not only compact size but also low cross-polarization and high frequency selectivity.

In this paper, a new type of SIW end-fire filtering antenna is proposed. It is composed of a vertically stacked SIW bandpass filtering circuit and an antipodal linearly tapered slot antenna (ALTSA). By using electric and magnetic mixed coupling structures, close-to-passband transmission zeros are generated and

flexibly adjustable. Commercial software ANSYS HFSS is used to analyze and simulate the filtering antenna. For demonstration, two antenna prototypes operating at 30 GHz are designed, fabricated, and measured. Measured results show that both antenna prototypes provide good filtering performances and endfire radiation patterns simultaneously. Meanwhile, the proposed filtering antennas exhibit a rapid roll-off at the upper or lower edge of the passband due to the close-to-passband transmission zeros.
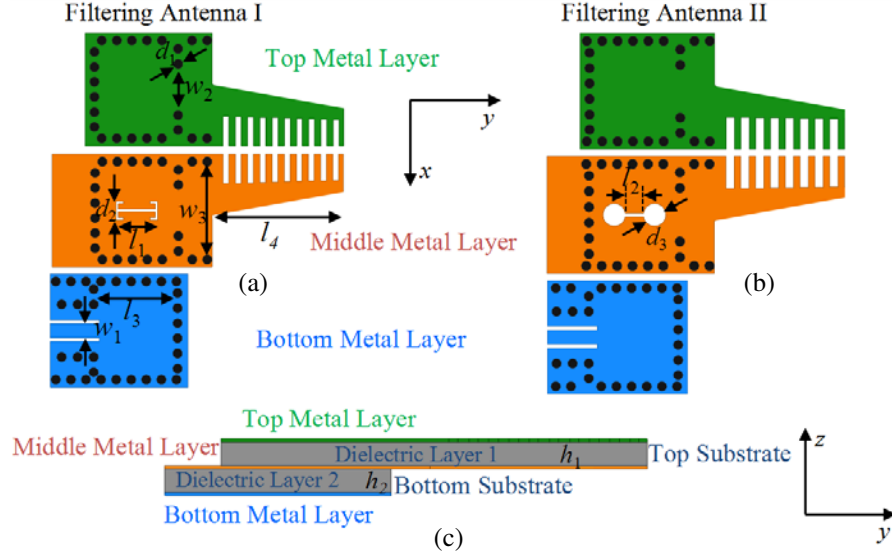
2. DESIGN AND ANALYSIS

Figure 1. Geometry of the proposed type of vertically stacked SIW filtering antenna.

The geometry of the SIW filtering antenna is illustrated in Fig. 1. It is a partially vertically stacked structure, which is composed of a SIW bandpass filtering circuit and a printed ALTSA. As shown, the filtering circuit consists of two vertically stacked SIW cavity resonators. The cavity in the bottom substrate, fed by a coplanar waveguide (CPW) line on the bottom metal layer, constitutes the first resonator of the filtering circuit. The cavity in the top substrate constitutes the second resonator of the filtering circuit. The internal coupling between these two cavity resonators is realized through a slot on the middle metal layer. The ALTSA printed on the top substrate is fed by a SIW-to-slotline transition. And the periodically arranged slits along the ALTSA edge are used to minimize the backward radiation [9]. For this type of filtering antenna, by introducing electric and magnetic mixed coupling between the cavity resonators, a second-order bandpass filtering characteristic with controllable transmission zeros can be achieved. The mixed coupling refers to the existence of the magnetic field and electric field coupling between adjacent resonators. The coupling reactance between the resonators can be expressed as [10].

$$M(\omega) = \omega L_m - \frac{1}{\omega C_m} \tag{1}$$

where L_m and C_m represent the coupling inductance and capacitance, respectively. By assuming $\omega/\omega_0 = 1$ for narrowband bandpass approximation ($\omega_0 = 1/\sqrt{LC}$ is the resonant frequency), a temporary coupling function N can be defined as

$$N = \frac{M(\omega_0)}{\omega_0 L} = \frac{L_m}{L} - \frac{C}{C_m} = M_c - E_c \tag{2}$$

where M_c represents the magnetic coupling coefficient, and E_c represents the electric coupling coefficient.

Then, the mixed coupling coefficient k can be expressed as

$$k = \frac{M_c - E_c}{1 - M_c E_c} \qquad (3)$$

If $k > 0$ the magnetic field coupling (inductive coupling) is dominant, and if $k < 0$ the electric field coupling (capacitive coupling) is dominant. By properly choosing the structure of the coupling slot, electrical and magnetic coupling can coexist between adjacent resonators to produce transmission zeros, resulting in a good selectivity. Moreover, the location of the transmission zeros can be flexibly controlled by adjusting the dimensions and shape of the coupling slot. For vertically stacked SIW structures, rectangular and circular slots are always used to achieve coupling between adjacent layers. In a rectangular SIW cavity resonator, the specific position of the coupling slot can be determined according to the electric field or magnetic field distribution in the resonant cavity. Fig. 2 shows the field distributions of TE_{101} mode in a rectangular SIW cavity resonator. As shown, near the center of the cavity, the electric field is strong, but the magnetic field is relatively weak. On the contrary, close to the edge of the cavity, the magnetic field is stronger, but the electric field is weaker. In principle, the coupling slot will be arranged on the position where the electric field or magnetic field is relatively strong [11].
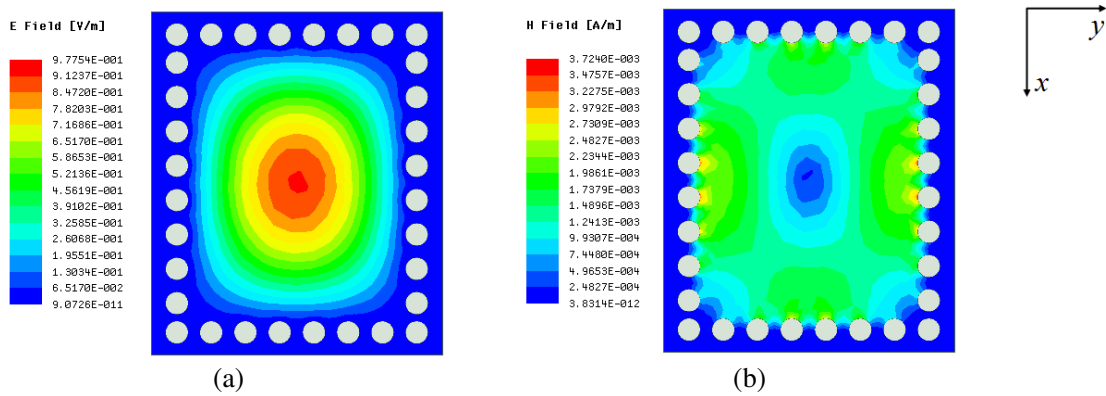

(a)   (b)

Figure 2. The field distributions of TE_{101} mode in a rectangular SIW cavity. (a) E-field. (b) H-field.

To verify our ideas, two prototypes of filtering antenna operating at 30 GHz are designed (see Fig. 1). By properly choosing the shape and dimensions of the coupling slots, either magnetic or electric coupling can be dominant. Fig. 1(a) presents the modified H-shaped slot coupling structure where the mixed-coupling is electric, which introduces a transmission zero at the lower side of the resonant frequency of TE_{101} mode. Fig. 3 shows the simulated realized gains of the filtering antenna I with different values of length l_1. As shown, the bandwidth of the passband and the location of transmission zero can be controlled by varying the value of length l_1. It can be observed from Fig. 3 that the bandwidth gradually increases with an increasing length l_1. And the transmission zero deepens as the length l_1 decreases. It is worth noting that although the bandwidth and transmission-zero location have changed, the transmission zero is always located on the lower side of the passband, because electric coupling is always dominate.

Furthermore, when the dumbbell-shaped slot coupling structure (see Fig. 1(b)) is used, the mixed-coupling becomes magnetic, and a transmission zero is then generated at the upper side of the resonant frequency of TE_{101} mode. Fig. 4 shows the simulated realized gains of the filtering antenna II with different values of length l_2. It is seen that the bandwidth of the passband and the location of transmission zero can be controlled by varying the value of length l_2. As shown, the bandwidth gradually decreases with an increasing length l_2. And the location of transmission zero shifts towards lower frequencies as the length l_2 increases. In addition, since magnetic coupling is always dominant, transmission zeros are always located on the upper edge of the passband.

It should be pointed out that, in this paper, we judge the properties of mixed-coupling by the simulated results. Fig. 5 gives the simulated phase curve of S_{21} of the filtering structure in filtering
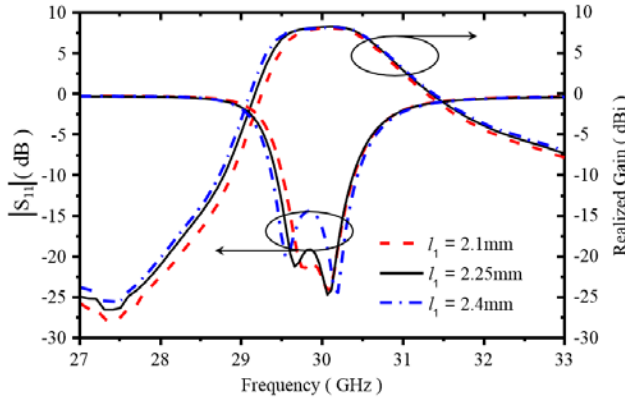
Figure 3. Simulated reflection coefficients and realized gains of the filtering antenna I with different values of l_1.
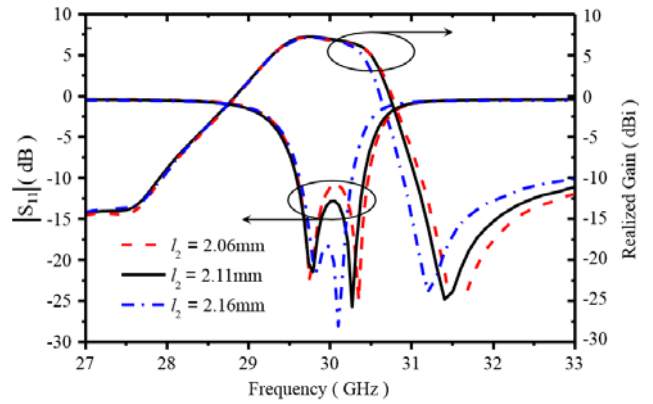

Figure 4. Simulated reflection coefficients and realized gains of the filtering antenna II with different values of l_2.
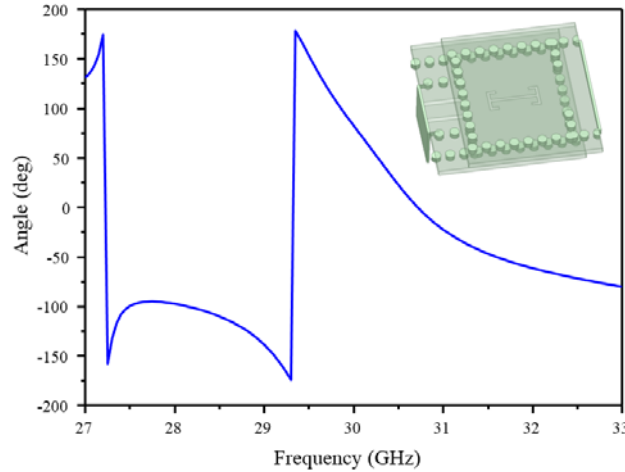

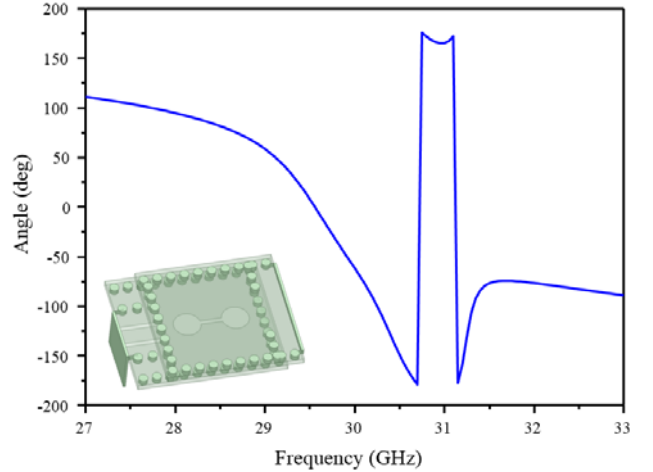**Figure 5.** Simulated phase curve of S_{21} of the filtering structure in filtering antenna I.

Figure 6. Simulated phase curve of S_{21} of the filtering structure in filtering antenna II.

antenna I. It can be seen that when the modified H-shaped slot coupling structure is adopted, the phase of S_{21} near the center frequency is positive (about 90 degrees), which means that the capacitive coupling is dominant. Therefore, in this case the mixed-coupling is electric. Fig. 6 shows the simulated phase curve of S_{21} of the filtering structure in filtering antenna II. It is seen that when the dumbbell-shaped slot coupling structure is used, the phase of S_{21} near the center frequency is negative, which means the inductive coupling is dominant, therefore the mixed-coupling is magnetic. It should be noted that, for the location of transmission zeros, due to the use of different resonator structures, the conclusion is contrary to the reference [10].

3. RESULTS AND DISCUSSION

To validate the design, the proposed vertically stacked SIW filtering antennas are fabricated and measured. Fig. 7 shows one of the photographs of the fabricated filtering antennas. Both layers of the vertically stacked filtering antennas are realized on a Rogers RT/Duriod 5880 substrate with the relative permittivity of 2.2, thickness of 0.254 mm, and loss tangent of 0.0009. Commercial software ANSYS HFSS is used to optimize the filtering antennas. The final dimensions are listed in Table 1.

Table 1. Design parameters of the filtering antennas (in units of mm).

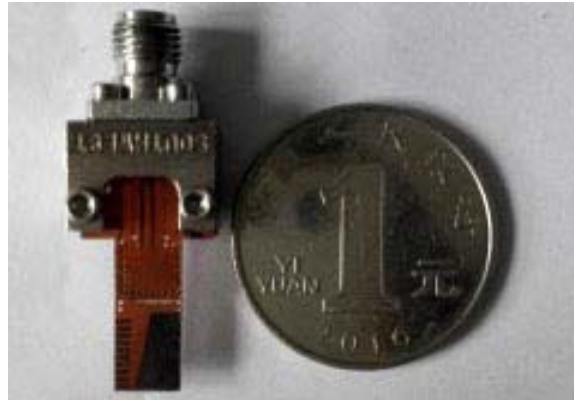| $l_1 = 1.96$	$l_2 = 0.95$	$l_3 = 4.1$	$l_4 = 7.0$
$w_1 = 0.72$	$w_2 = 2.38$	$w_3 = 4.8$	$d_1 = 0.4$
$d_2 = 1.0$	$d_3 = 1.2$	$h_1 = 0.254$	$h_2 = 0.254$

Figure 7. Photograph of the fabricated filtering antenna.

The simulated and measured reflection coefficients and realized gains of the proposed filtering antennas (I and II) are illustrated in Fig. 8. As shown, good agreement between the simulated and measured results is observed, with the discrepancy mainly due to the fabrication tolerance and experimental imperfection. The measured 3-dB fractional bandwidths (FBWs) of filtering antenna I and II are 4.43% (29.56–30.90 GHz) and 4.64% (29.24–30.63 GHz), respectively. With reference to the gain curves, good bandpass filtering responses are achieved. At the operating frequency of 30 GHz, the realized gain is measured to be 7.57 dBi and 7.49 dBi, respectively. Meanwhile, the transmission zero clearly appear on the lower or upper side of the passband of the filtering antennas I or II, respectively, resulting in good selectivity. It is worth mentioning that, in this paper, the mixed-coupling method is used to introduce one transmission zero at the upper or lower side of the passband, leading to an
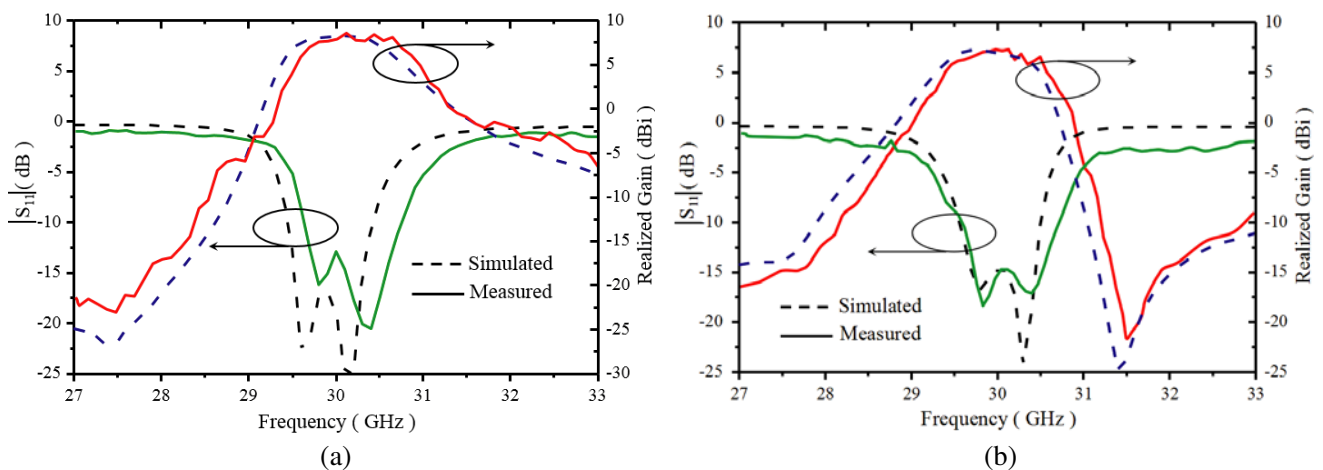

Figure 8. Simulated and measured reflection coefficients and realized gains of the filtering antennas. (a) Filtering antenna I. (b) Filtering antenna II.
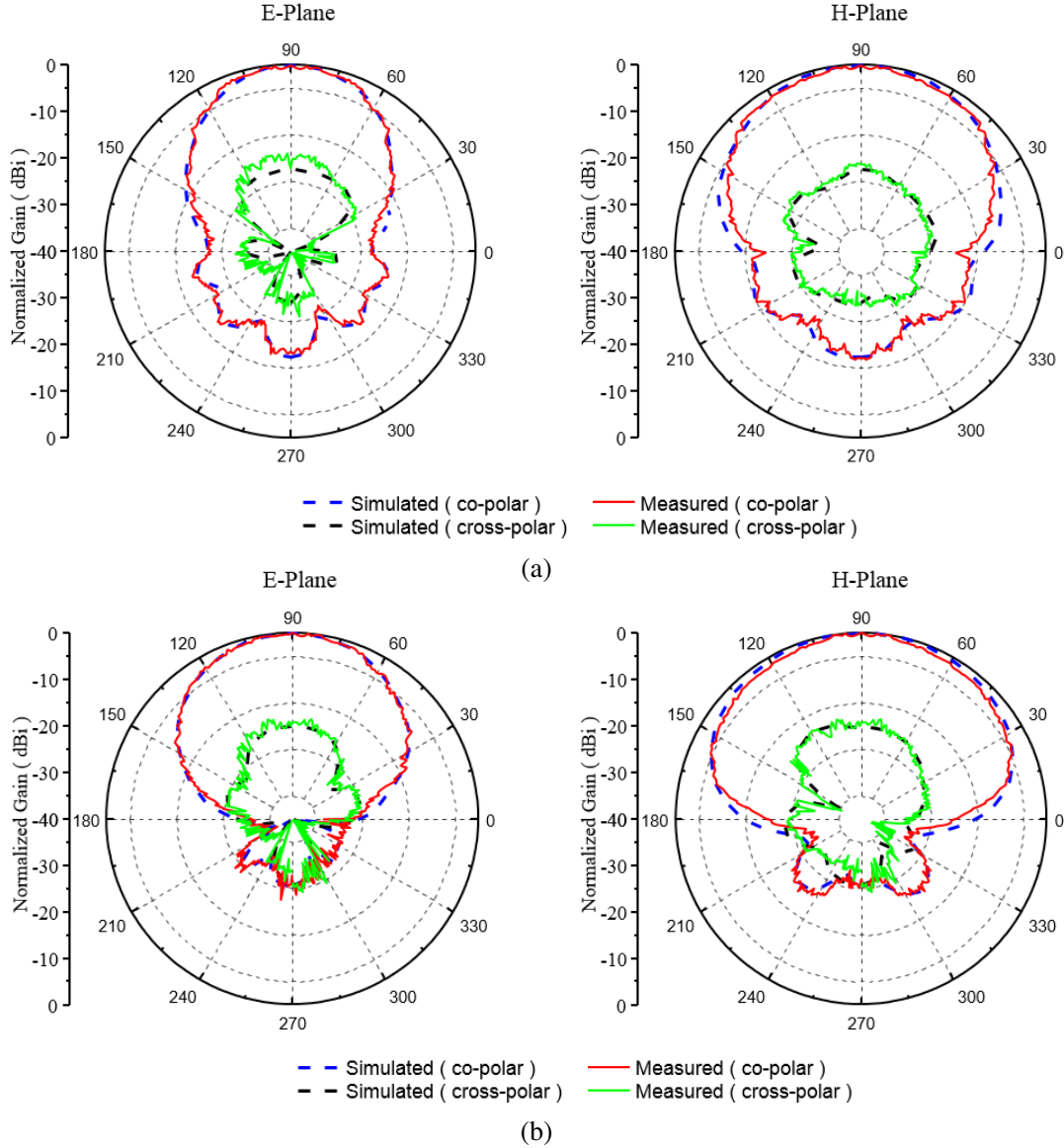
E-Plane   H-Plane

Figure 9. Simulated and measured radiation patterns of the filtering antennas. (a) Filtering antenna I. (b) Filtering antenna II.

asymmetric filtering characteristic. Furthermore, the source-to-load coupling method in [3] may be used to generate two transmission zeros.

Figure 9(a) shows the simulated and measured normalized radiation patterns of the filtering antenna I in the two orthogonal planes (E- and H-planes) at 30 GHz. It is observed that endfire radiation patterns are obtained. The simulated and measured results agree well with each other, exhibiting a maximum radiation in the endfire direction. The measured 3-dB beamwidths are $52.5°$ and $89.2°$ in the E- and H-planes, respectively. The measured co-polar fields are 19.2 dB stronger than the cross-polar counterparts. Meanwhile, the measured front-to-back ratios are more than 16.1 dB. The difference between the simulated and measured radiation patterns is mainly due to the influence of the fixture, screws, and feed setup including K Type Connector and cable near the antenna under test. Fig. 9(b) gives the simulated and measured radiation patterns of filtering antenna II, which exhibits similar radiation patterns to filtering antenna I. The measured 3-dB beamwidths are $63.7°$ and $99.8°$ in the E- and H-planes, respectively. The cross-polarization levels are better than 17.5 dB in the two orthogonal planes. And the measured front-to-back ratios are more than 18.4 dB.

4. CONCLUSION

A new type of vertically stacked SIW filtering antenna has been presented in this paper. By using a SIW bandpass filtering circuit together with the printed ALTSA, a second-order filtering characteristic has been achieved. The mixed coupling structures have been adopted, which introduced a flexibly controllable transmission zero close to the passband. For demonstration, two antenna prototypes operating at 30 GHz hav been designed, fabricated, and measured. Measured results show that the antenna prototypes provide both good filtering performances and endfire radiation patterns simultaneously. For both antenna prototypes, due to the existence of the transmission zeros, the gain drops significantly near the passband edge leading to high frequency selectivity.

ACKNOWLEDGMENT

REFERENCES

1. Chuang, C.-T. and S.-J. Chung, "Synthesis and design of a new printed filtering antenna," *IEEE Trans. Antennas Propag.*, Vol. 59, No. 3, 1036–1042, 2011.

2. Lin, C.-K. and S.-J. Chung, "A compact filtering microstrip antenna with quasi-elliptic broadside antenna gain response," *IEEE Antennas Wirel. Propag. Lett.*, Vol. 10, 381–384, 2011.

3. Dhwaj, K., J. M. Kovitz, H. Tian, L. J. Jiang, and T. Itoh, "Half-mode cavity based planar filtering antenna with controllable transmission zeros," *IEEE Antennas Wirel. Propag. Lett.*, Vol. 17, 833–836, 2018.

4. Hua, C., R. Li, Y. Wang, and Y. Lu, "Dual-polarized filtering antenna with printed jerusalem-cross radiator," *IEEE Access*, Vol. 6, 9000–9005, 2018.

5. Lu, Y.-L, Y. Wang, S. Gao, C. Hua, and T. Liu, "Circularly polarized integrated filtering antenna with polarisation reconfigurability," *IET Antennas Propag.*, Vol. 11, No. 15, 2247–2252, 2017.

6. Yusuf, Y., Cheng, H., and X. Gong, "A seamless integration of 3-D vertical filters with highly efficient slot antennas," *IEEE Trans. Antennas Propag.*, Vol. 59, No. 11, 4016–4022, 2011.

7. Cheng, H., Yusuf, Y., and X. Gong, "Vertically integrated three-pole filter/antennas for array applications," *IEEE Antennas Wirel. Propag. Lett.*, Vol. 10, 278–281, 2011.

8. Shi, J., X. Wu, Z. N. Chen, X. Qing, L. Lin, J. Chen, and Z.-H. Bao, "A compact differential filtering quasi-Yagi antenna with high frequency selectivity and low cross-polarization levels," *IEEE Antennas Wirel. Propag. Lett.*, Vol. 14, 1573–1576, 2015

9. Hua, C., X. Wu, N. Yang, and W. Wu, "Air-filled parallel-plate cylindrical modified Luneberg lens antenna for multiple-beam scanning at millimeter-wave frequencies," *IEEE Trans. Microw. Theory Techn.*, Vol. 61, No. 1, 436–443, 2013.

10. Chu, Q.-X. and H. Wang, "A compact open-loop filter with mixed electric and magnetic coupling," *IEEE Trans. Microw. Theory Techn.*, Vol. 56, No. 2, 431–439, 2008.

11. Yusuf, Y. and X. Gong, "Co-designed substrate-integrated waveguide filters with patch antennas," *IET Antennas Propag.*, Vol. 7, No. 7, 493–501, 2013.